
A Statistical Model for Dynamic Networks with Neural Variational Inference

Shubham Gupta

CSA Department
Indian Institute of Science
Bangalore, India.

Rui M. Castro

Department of Mathematics
Eindhoven University of Technology
Eindhoven, The Netherlands.

Ambedkar Dukkipati

CSA Department
Indian Institute of Science
Bangalore, India.

Abstract

In this paper we propose a statistical model for dynamically evolving networks, together with a variational inference approach. Our model, which we call Dynamic Latent Attribute Interaction Model (DLAIM), encodes edge dependencies across different time snapshots. It represents nodes via latent *attributes* and uses attribute *interaction matrices* to model the presence of edges. Both are allowed to *evolve* with time, thus allowing us to capture the *dynamics* of the network. We develop a neural network based variational inference procedure that provides a suitable way to learn the model parameters. The main strengths of DLAIM are: **(i)** it is flexible as it does not impose strict assumptions on network evolution unlike existing approaches, **(ii)** it applies to both directed as well as undirected networks, and more importantly, **(iii)** learned node attributes and interaction matrices may be interpretable and therefore provide insights on the mechanisms behind network evolution. Experiments done on real world networks for the task of link forecasting demonstrate the superior performance of our model as compared to existing approaches.

1 INTRODUCTION

Network analysis is by no means a new field and consequently a towering wealth of literature that explores various aspects of network analysis is available (Goldenberg et al., 2010). However, as opposed to static networks, the study of *dynamic* or *temporally evolving* networks is still in a nascent stage. But over the past few years, due to emergence of exciting applications and advancements in computing capabilities, the study

of dynamic networks has witnessed a steady progress with a positive acceleration (Kim et al., 2017).

A naive way to study dynamic networks is by applying static network analysis techniques to each individual network *snapshot*. However, this approach implicitly assumes that each snapshot has independent information, and completely ignores the relationship and shared information between snapshots. Those relationships are the essence of the network evolution, and both modeling and understanding them is of paramount importance. The situation is analogous to predicting the position of a car based on observed noisy positions from the past. Methods that ignore the dynamics of a moving vehicle perform rather poorly in comparison to methods that take it into account.

When one considers a dynamic network, both the presence of edges as well as nodes may vary over time. However, in many real-world contexts it is reasonable to assume that the number of nodes is fixed over time (i.e. no new node joins the network and no existing node leaves it). Protein-protein interaction networks are one such type of networks. In this paper, our main focus is on networks for which the presence of nodes is invariant over time while the presence of edges is time dependent. In Appendix D, we also outline an extension of our approach that accommodates the *birth* and *death* of nodes as well.

In this paper, we propose a statistical model for dynamic networks, which we call Dynamic Latent Attribute Interaction Model (DLAIM). This model imposes a minimal set of assumptions on the dynamics, in contrast with other existing approaches (Xing et al., 2010; Foulds et al., 2011; Heaukulani & Ghahramani, 2013; Kim & Leskovec, 2013; Gupta et al., 2019). This increases the flexibility of our model. Furthermore, our model applies to directed as well as undirected networks. Rather than focusing on a specific inference task, our model attempts to capture some of the mechanisms believed to be behind the network evolution. This means that performing inference in this

model can give important insights about the network evolution. In particular, our model is able to capture underlying community structures and evolving node attributes and their interactions.

In theory, the parameters of the proposed model could be estimated (from training data) via Bayesian inference. However, the likelihood structure of the model is complex and non-convex, making such methods computationally infeasible. This motivates a neural network based variational inference procedure yielding an end-to-end trainable architecture that can be used for efficient and scalable inference. This is described in detail in Sections 3 and 4.

To objectively compare the performance of our model to existing approaches we consider the task of link forecasting - predicting future network links given only the past observations. Perhaps more interestingly (although more subjective) one can examine the learned node attributes and interactions and their evolution. Notably, in Section 5.2 we show that the learned quantities may have a physical significance, providing insights in line with what one expects given the knowledge and context of these networks (collaboration networks in our examples). These might be used as aids for visualization, as well as for interpretation of network dynamics.

Contributions: (i) we have proposed a new statistical model for dynamic networks that encodes temporal edge dependencies and can model both undirected and directed networks; (ii) we have developed a computationally scalable neural network based variational inference procedure for the model; and (iii) we have provided ample empirical evidence that the model is suitable for link forecasting while simultaneously providing important insights into the network evolution mechanics as it can provide interpretable embeddings.

2 RELATED WORK

One of the first successful statistical model for dynamic networks was proposed in (Xing et al., 2010). It is an extension of the well known Mixed Membership Stochastic Blockmodel (Airoldi et al., 2008) with the additional assumption that parameters evolve via a Gaussian random walk, i.e. $\boldsymbol{\mu}^{(t)} \sim \mathcal{N}(\mathbf{A}\boldsymbol{\mu}^{(t-1)}, \boldsymbol{\Phi})$, where $\boldsymbol{\mu}^{(t)}$ is a parameter and \mathbf{A} and $\boldsymbol{\Phi}$ are fixed matrices. Since \mathbf{A} and $\boldsymbol{\Phi}$ are fixed, the model assumes that the process governing the network dynamics itself does not change over time, which might be a limiting assumption. Since then, multiple researchers have proposed extensions of static network models like Stochastic Blockmodel (Holland et al., 1983) to the case of dynamic networks (Yang et al., 2011; Xu & Hero, 2014; Xu, 2015).

Another class of models extend the general latent space model for static networks to the dynamic network setting (Sarkar & Moore, 2005; Foulds et al., 2011; Heaukulani & Ghahramani, 2013; Kim & Leskovec, 2013; Sewell & Chen, 2015, 2016; Gupta et al., 2019). Our proposed model also falls under this category. The basic idea behind such models is to represent each node by an embedding (which may change with time) and model the probability of an edge as a function of the embeddings of the two endpoints. All of these approaches (except (Gupta et al., 2019)) use an MCMC based inference procedure that does not directly support neural network based inference.

Our model most closely resembles (Kim & Leskovec, 2013) in terms of modeling network snapshots and (Gupta et al., 2019) in terms of performing inference. However, there are notable differences: (i) approaches like (Sarkar & Moore, 2005; Foulds et al., 2011; Kim & Leskovec, 2013; Sewell & Chen, 2015) assume that the nature of interactions between nodes is constant over time. In our model the role of each attribute can also change. This is a rather distinctive feature of DLAIM, allowing us to capture both local dynamics (the evolution of node attributes) and global dynamics (the evolving role of attributes); (ii) our model for static network snapshots is fully differentiable which allows us to use a neural network based variational inference procedure as opposed to most existing methods that use MCMC based inference; (iii) approaches like (Xing et al., 2010; Heaukulani & Ghahramani, 2013; Gupta et al., 2019) impose strict restrictions on dynamics, for example, (Heaukulani & Ghahramani, 2013; Gupta et al., 2019) assume that each attribute changes based on a non-negative linear combination of its neighbors. This is not necessarily justified in all settings. In DLAIM we assume only a smoothly changing network; and (iv) since we do not use the adjacency matrix row as input to our neural network, our model is more scalable as compared to (Gupta et al., 2019)

3 DYNAMIC LATENT ATTRIBUTE INTERACTION MODEL

3.1 Modeling Individual Snapshots

In our model, time $t \in \{1, 2, \dots, T\}$ is discrete. The network evolution is therefore described by the corresponding network snapshots at each timestep specified by binary adjacency matrices $\mathbf{A}^{(t)} \in \{0, 1\}^{N \times N}$ where N is the number of nodes. We assume that there are no self-loops. Each node is modeled by K latent *attributes* whose values lie in the interval $[0, 1]$. These attributes can change over time. We use $\mathbf{z}_n^{(t)} \in [0, 1]^K$ to denote the latent attributes of node n at time t .

The interaction between the attribute vectors of each pair of nodes directly dictates the probability of observing an edge between them. For simplicity, our interaction model only encodes interactions between attributes of the same type, described by *interaction matrices*. Let $\Theta_k^{(t)} \in \mathbb{R}^{2 \times 2}$, be a matrix that encodes the affinity between nodes with respect to attribute k at time t . For undirected graphs, the matrices $\Theta_k^{(t)}$ are symmetric. At time t the node attributes and interaction matrices fully determine the probability of edges being present. Formally, given $\Theta_k^{(t)}$, $k = 1, \dots, K$ and $\mathbf{z}_n^{(t)}$, $n = 1, \dots, N$, edges occur independently and the probability of an edge from node i to j is modeled as:

$$P(a_{ij} = 1 | \mathbf{z}_i^{(t)}, \mathbf{z}_j^{(t)}, \{\Theta_k^{(t)}\}_{k=1}^K) = \sigma\left(\sum_{k=1}^K \tilde{\theta}_k^{(t)}(i, j)\right), \quad (1)$$

where, $\tilde{\theta}_k^{(t)}(i, j)$ is defined as:

$$\tilde{\theta}_k^{(t)}(i, j) = \mathbb{E}_{x \sim B(z_{ik}^{(t)}), y \sim B(z_{jk}^{(t)})} [\Theta_k^{(t)}(x, y)]. \quad (2)$$

Here $\sigma(\cdot)$ is the *sigmoid* function, $B(\alpha)$ refers to a Bernoulli distribution with parameter α and $\Theta_k^{(t)}(x, y)$ is the $(x, y)^{th}$ entry of $\Theta_k^{(t)}$ matrix. Finally x and y are independent. This formulation allows representation of both homophilic and heterophilic interactions among nodes based on the structure of matrices $\Theta_k^{(t)}$.

The interaction model that we consider is in the same spirit as the Multiplicative Attribute Graph (MAG) model (Kim & Leskovec, 2012). Some other dynamic network models (Kim & Leskovec, 2013) use the MAG model directly to represent each static network snapshot, however, in our case we have a few differences: our node attributes are not restricted to being binary and; we have a differentiable expectation operation as given in (2) instead of the non-differentiable ‘‘selection’’ operation given in (Kim & Leskovec, 2012). These differences crucially allow us to use a neural network based variational inference procedure.

3.2 Modeling Network Dynamics

Having described how each network snapshot is generated, it remains to describe how attributes and their interactions evolve over time. To make an analogy with genetics, each attribute type might be seen as a *gene*, and the attribute vector corresponds to the *gene expression profile* of a given node. The level of expression of each attribute might change over time - nodes may start exhibiting new attributes and stop exhibiting old ones thereby leading to a change in $\mathbf{z}_n^{(t)}$. At the same time, the role of each attribute in regulating the presence of edges in the network may also change over time leading to a change in $\Theta_k^{(t)}$ matrices.

One approach to model the dynamics of a network is to use domain expertise to impose a specific set of assumptions on the process governing the dynamics. However, this limits the class of networks that can be faithfully modeled. Instead, we adopt the strategy of imposing a minimal set of assumptions on the dynamics. This is in the same spirit as in the models used in tracking using stochastic filtering (e.g., Kalman filters) (Yilmaz et al., 2006), where dynamics are rather simple and primarily capture the insight that the state of the system cannot change too dramatically over time. The use of simple dynamics together with a powerful function approximator (a neural network) during the inference ensures that a simple yet powerful model can be learned from observed network data.

Let $\bar{\theta}_k^{(t)}$ be a vector consisting of the entries of $\Theta_k^{(t)}$ matrix¹. We model the evolution of matrices $\Theta_k^{(t)}$ as:

$$\bar{\theta}_k^{(t)} \sim \mathcal{N}(\bar{\theta}_k^{(t-1)}, s_{\theta}^2 \mathbf{I}) \quad k = 1, \dots, K, \quad t = 2, \dots, T, \quad (3)$$

where $s_{\theta}^2 \in \mathbb{R}^+$ is a model hyperparameter and \mathbf{I} denotes the identity matrix. This model captures the intuition that the interaction matrices will likely not change dramatically over time.

Since the entries of the attribute vector $\mathbf{z}_n^{(t)}$ are restricted to lie in $[0, 1]$ a similar dynamics model as above is not possible. A simple workaround is to reparameterize the problem by introducing the vectors $\psi_n^{(t)} \in \mathbb{R}^K$ such that

$$z_{nk}^{(t)} = \sigma(\psi_{nk}^{(t)}). \quad (4)$$

As before, $\sigma(\cdot)$ is the sigmoid function. Now we can have an evolution model similar to (3) on vectors $\psi_n^{(t)}$:

$$\psi_n^{(t)} \sim \mathcal{N}(\psi_n^{(t-1)}, s_{\psi}^2 \mathbf{I}) \quad n = 1, \dots, N, \quad t = 2, \dots, T. \quad (5)$$

Here s_{ψ}^2 is a model hyperparameter. This in turn models the evolution of vectors $\mathbf{z}_n^{(t)}$.

Note that (3) and (5) only imply that the values of variables are unlikely to change very quickly. Other than that, they do not place any strong or network specific restriction on the dynamics. The hyperparameters s_{θ}^2 and s_{ψ}^2 control the magnitude of likely change.

This approach for modeling dynamics has advantages and disadvantages. The major advantage is flexibility, since during inference time, a powerful enough function approximator can learn appropriate network dynamics from the observed data. However, this is a generative model and realizations of this model will

¹For directed graphs the matrix $\Theta_k^{(t)}$ can be arbitrary, therefore $\bar{\theta}_k^{(t)}$ will have four entries. For undirected graphs the matrices are symmetric, and hence three entries suffice.

generally yield globally unrealistic network dynamics. Nevertheless, within small time intervals, the behavior of the networks will be consistent with what is observed in realistic scenarios, and this is enough to ensure good tracking performance. In many real world cases, a suitable amount of observed data is available but clues about the network dynamics are unavailable. Since the task is to gain meaningful insights from the data, we believe the advantages of this approach outweigh the disadvantages.

Note that (3) and (5) are applicable from timestep 2 onward. The initial vectors $\psi_n^{(1)}$ and $\bar{\theta}_k^{(1)}$ are sampled from the following prior distributions:

$$\bar{\theta}_k^{(1)} \sim \mathcal{N}(\mathbf{0}, \sigma_{\bar{\theta}}^2 \mathbf{I}), \quad \psi_n^{(1)} \sim \mathcal{N}(\mathbf{0}, \sigma_{\psi}^2 \mathbf{I}). \quad (6)$$

Here, σ_{θ} and σ_{ψ} are hyperparameters. In our experiments, we set these hyperparameters to a high value ($\sigma_{\theta} = \sigma_{\psi} = 10$). This allows the initial embeddings to become flexible enough to represent the first snapshot faithfully. After that, the assumption that the network changes slowly ((3) and (5)) is used to sample the value of random variables $\psi_n^{(t)}$ and $\bar{\theta}_k^{(t)}$ for $t = 2, 3, \dots, T$.

We make the following independence assumptions: given $\psi_n^{(t-1)}$ the vectors $\psi_n^{(t)}$ are independent of any quantity indexed by time $t' \leq t - 1$. An analogous statement applies to the interaction matrices $\bar{\theta}_k^{(t)}$. Finally, given $\psi_i^{(t)}$, $\psi_j^{(t)}$ and $\bar{\Theta}^{(t)} = \{\bar{\theta}_k^{(t)}\}_{k=1}^K$, the entries $a_{ij}^{(t)}$ are independent of everything else. The graphical model and generative process for DLAIM are given in Fig. 3 and Algorithm 1 respectively in Appendix A.

4 INFERENCE IN DLAIM

In practice an observed sequence of network snapshots $\mathbf{A} = [\mathbf{A}^{(1)}, \mathbf{A}^{(2)}, \dots, \mathbf{A}^{(T)}]$ is available, and the main inference task is to estimate the values of the underlying latent random variables. In DLAIM performing exact inference is intractable because the computation of marginalized log probability of observed data results in integrals that are hard to evaluate. Thus, approximate inference techniques must be adopted.

Our goal is to compute an approximation to the true posterior distribution $P(\{\Psi^{(t)}, \Theta^{(t)}\}_{t=1}^T | \{\mathbf{A}^{(t)}\}_{t=1}^T)$. Note that, in our current approach K , s_{θ} , s_{ψ} , σ_{θ} and σ_{ψ} are hyperparameters, that are simply set by the user. We pose the inference problem as an optimization problem by using Variational Inference (Blei et al., 2017) and parameterize the approximating distribution by a neural network. There are several benefits like efficiency and scalability (Blei et al., 2017) associated with the use of variational inference. Also, coupled with powerful neural networks, the ability of variational inference to model complicated distributions

has been demonstrated by several researchers (Kingma & Welling, 2013).

The main idea of variational inference is to approximate the posterior distribution by a suitable surrogate. Consider a general latent variable model with the set of all observed random variables \mathbf{X} and the set of all latent random variables \mathbf{H} . The (intractable) posterior distribution $P(\mathbf{H}|\mathbf{X})$ is approximated by using a parameterized distribution $Q_{\Phi}(\mathbf{H})$ where Φ is the set of all the parameters of Q . One would like the distribution Q to be as *close* to the distribution $P(\mathbf{H}|\mathbf{X})$ as possible. In general, Kullback-Leibler (KL) divergence is used as a measure of similarity between the two distributions. The goal of variational inference is to find the parameters Φ for which $\text{KL}(Q_{\Phi}(\mathbf{H})||P(\mathbf{H}|\mathbf{X}))$ is minimized. However, this optimization objective is intractable since one cannot efficiently compute $P(\mathbf{H}|\mathbf{X})$. Nevertheless one can show that maximizing the *Evidence Lower Bound Objective (ELBO)* given by

$$ELBO(\Phi) = \mathbb{E}_Q[\log P(\mathbf{X}, \mathbf{H}) - \log Q_{\Phi}(\mathbf{H})], \quad (7)$$

is equivalent to minimizing the KL criterion (Blei et al., 2017). For most models, the ELBO can be efficiently computed or approximated by imposing a suitable set of assumptions on Q as described later. In the context of our model the distribution Q will be parameterized by a neural network and hence Φ will represent the set of parameters of that neural network.

4.1 Approximating ELBO

The latent variables in our model correspond to the elements of $\Theta^{(t)}$ and $\Psi^{(t)}$ for $t = 1, 2, \dots, T$. The observed variables are $\mathbf{A}^{(1)}, \dots, \mathbf{A}^{(T)}$. The parameter vector Φ consists of the weights of the neural network. Following (7), we get:

$$ELBO(\Phi) = \mathbb{E}_Q[\log P(\{\mathbf{A}^{(t)}\}_{t=1}^T, \{\Psi^{(t)}, \Theta^{(t)}\}_{t=1}^T) - \log Q_{\Phi}(\{\Psi^{(t)}, \Theta^{(t)}\}_{t=1}^T)]. \quad (8)$$

Using the independence assumptions stated in Section 3, one can write:

$$\begin{aligned} \log P(\{\mathbf{A}^{(t)}\}_{t=1}^T, \{\Psi^{(t)}, \Theta^{(t)}\}_{t=1}^T) = & \sum_{n=1}^N \log P(\psi_n^{(1)}) + \sum_{k=1}^K \log P(\bar{\theta}_k^{(1)}) \\ & \sum_{t=2}^T \sum_{n=1}^N \log P(\psi_n^{(t)} | \psi_n^{(t-1)}) + \sum_{t=2}^T \sum_{k=1}^K \log P(\bar{\theta}_k^{(t)} | \bar{\theta}_k^{(t-1)}) \\ & + \sum_{t=1}^T \sum_{i \neq j} \log P(a_{ij}^{(t)} | \psi_i^{(t)}, \psi_j^{(t)}, \Theta^{(t)}). \end{aligned} \quad (9)$$

The right hand side of (9) can be computed using (1), (3), (4), (5) and (6). Following the standard practice (Blei et al., 2017), we also assume that $Q_{\Phi}(\cdot)$ belongs to a mean field family of distributions, i.e. all the variables are independent under Q :

$$Q_{\Phi}(\{\Psi^{(t)}, \Theta^{(t)}\}_{t=1}^T) = \left(\prod_{t=1}^T \prod_{n=1}^N q_{\psi_n}^{(t)}(\psi_n^{(t)}) \right) \left(\prod_{t=1}^T \prod_{k=1}^K q_{\bar{\theta}_k}^{(t)}(\bar{\theta}_k^{(t)}) \right). \quad (10)$$

We model the distributions $q_{\psi_n}^{(t)}$ and $q_{\bar{\theta}_k}^{(t)}$ using a Gaussian distribution as given in (11) and (12) (notation²).

$$q_{\psi_n}^{(t)}(\psi_n^{(t)}) = \mathcal{N}(\psi_n^{(t)} | \mathbf{m}_{\psi_n}^{(t)}, (\sigma_{\psi_n}^{(t)})^2 \mathbf{I}), \text{ and} \quad (11)$$

$$q_{\bar{\theta}_k}^{(t)}(\bar{\theta}_k^{(t)}) = \mathcal{N}(\bar{\theta}_k^{(t)} | \mathbf{m}_{\bar{\theta}_k}^{(t)}, (\sigma_{\bar{\theta}_k}^{(t)})^2 \mathbf{I}). \quad (12)$$

Here $(\sigma_x^{(t)})^2 \mathbf{I} = \text{diag}((\sigma_x^{(t)})_1^2, \dots, (\sigma_x^{(t)})_{|x|}^2)$. We wish to learn the mean and covariance parameters of Gaussian distributions in (11) and (12) (these are called *variational parameters*). There are two possible approaches for doing this: **(i)** $ELBO(\Phi)$ can be directly optimized as a function of variational parameters or **(ii)** One can model the variational parameters as outputs of some other parametric function (like a neural network) and then optimize the parameters of that parametric function. The second approach can be viewed as a form of regularization where the space in which variational parameters can lie is constrained to the range of the parametric function in use. We adopt the latter approach, and obtain the variational parameters as outputs of neural networks. We use Φ to denote the set of neural network parameters. Thus $q_{\psi_n}^{(t)}(\psi_n^{(t)}) \equiv q_{\psi_n}^{(t)}(\psi_n^{(t)}; \Phi)$, but we do not explicitly mention the dependence on Φ in general to avoid notational clutter. $ELBO(\Phi)$ can now be computed by using (9) and (10) in (8). Integration of the term involving $\log P(a_{ij}^{(t)} | \psi_i^{(t)}, \psi_j^{(t)}, \Theta^{(t)})$ is hard, so for this term Monte Carlo estimation can be used. In all our experiments we use only one sample to get an approximation to (8) as it was done in (Kingma & Welling, 2013). Additionally, we empirically observed that for $t = 1$, using $\mathbf{m}_{\psi_n}^{(1)}$ and $\bar{\theta}_k^{(1)}$ directly as a sample for Monte-Carlo estimation improves the link forecasting performance and hence we do this in our experiments.

4.2 Network Architecture

We use a neural network to parameterize the distributions in (11) and (12). Our network consists of four

separate GRUs (Cho et al., 2014) (also see Appendix C), one each for the mean and covariance parameters (\mathbf{m}_{ψ} , σ_{ψ} , $\mathbf{m}_{\bar{\theta}}$ and $\sigma_{\bar{\theta}}$). Details about network architecture are given in Appendix B.

Once the mean and covariance parameters are available, we use the reparameterisation trick (Kingma & Welling, 2013) to sample $\psi_n^{(t)}$ and $\bar{\theta}_k^{(t)}$ using (11) and (12) which are then used to approximate $ELBO(\Phi)$ using (8) as described in Section 4.1. The training objective is to maximize $ELBO(\Phi)$. The beauty of our model is that $ELBO(\Phi)$ is differentiable with respect to Φ and gradients can be easily computed by back-propagation which allows one to capitalize on the powerful optimization methods used for training neural networks. Furthermore, since ELBO uses only pairwise interactions among nodes, we can operate in a batch setting where only a subset of all nodes and the interactions within this subset are considered. This allows us to scale up to rather large networks by training our model on random batches of nodes.

One additional benefit of using a neural network as opposed to learning the variational parameters directly is that the neural network should be able to capture the temporal patterns in the data that cannot be captured by the variational parameters on their own. Since the neural network is being trained to predict the parameters for time t given the history up to time $t - 1$, it is being encouraged to look for temporal patterns.

We use the well known Adam optimizer (Kingma & Ba, 2014) with a learning rate of 0.01 to train the inference network. A separate inference network is trained for all time steps (in other words, to make predictions for time t we train the inference network with all the observations up to time $t - 1$). Note that all networks have exactly the same number of parameters. When training, parameters of the neural network that is used to make predictions at time t are initialized with the parameters of trained network for time $t - 1$.

A Note on Scalability: For each batch/iteration, one needs edge probabilities and distance between embeddings across successive timesteps. These require $O(b^2KT)$ and $O(bKT)$ operations, respectively ($b = \text{batch size}$). Note, however, that many operations can be parallelized to improve runtime. We use $b = \min(N, 256)$ and randomly sample 1000 – 3000 batches in our experiments. Moreover, approaches that use MCMC are usually much slower than approaches that use variational inference (Blei et al., 2017) and hence we believe that our approach is more scalable as compared to existing approaches.

²Define $\mathcal{N}(\mathbf{x} | \boldsymbol{\mu}, \boldsymbol{\Sigma}) = \frac{1}{(2\pi^{|\boldsymbol{\Sigma}|})^{|\boldsymbol{\mu}|/2}} \exp(-\frac{1}{2}d(\mathbf{x}, \boldsymbol{\mu}))$, where $d(\mathbf{x}, \boldsymbol{\mu}) = (\mathbf{x} - \boldsymbol{\mu})^\top \boldsymbol{\Sigma}^{-1}(\mathbf{x} - \boldsymbol{\mu})$

Table 1: Dataset Description

Dataset	#Nodes	#Snapshots	Directed
Enron-50	50	37	✗
Enron-Full	149	24	✓
Infocom	78	50	✗
NIPS-110	110	17	✗
EU-U	986	33	✗
EU-D	986	33	✓
CollegeMsg	1899	19	✓
MIT Reality Mining	94	37	✗

5 EXPERIMENTS

In this section, we evaluate the performance of our model on several benchmark real world networks. In order to objectively compare the performance of DLAIM with other approaches we focus on the task of link forecasting (formally described in Section 5.1). In these examples our approach outperforms other approaches suitable for this task. We also perform a qualitative case study to demonstrate the utility of learned node attribute vectors and interaction matrices. Table 1 summarizes the datasets (also see Appendix E).

5.1 Link Forecasting

We consider the setting where we are given a dynamic network up to timestep T as a sequence of snapshots, $[\mathbf{A}^{(1)}, \mathbf{A}^{(2)}, \dots, \mathbf{A}^{(T)}]$. The task is to use the observed data to predict $\mathbf{A}^{(T+1)}$. Note that this task is different (and inherently more difficult) from *missing link prediction* where only missing edges at timestep T are to be found.

In all our experiments, we fixed the value of $K = 32$ as it allowed significant amount of flexibility to the model while maintaining computational tractability. Similarly, based on preliminary experiments with NIPS-110 dataset, we chose $s_\theta = s_\psi = 0.1$ and $\sigma_\theta = \sigma_\psi = 10$ for all experiments. The fact that we were able to reuse the same values of hyperparameters across all our link forecasting experiments indicates that our approach is rather robust and dataset specific tuning is not generally required.

A simple baseline method (denoted by BAS) treats each entry of $\mathbf{A}^{(T+1)}$ as an independent Bernoulli random variable with a *Beta*(1,1) prior (Foulds et al., 2011). We compare our performance against this simple baseline and other existing approaches (Miller et al., 2009; Foulds et al., 2011; Kim & Leskovec, 2013; Gupta et al., 2019).

LFRM or Latent Feature Infinite Relational Model

(Miller et al., 2009) represents nodes in a static network using binary feature vectors. It is a non-parametric model. It imposes Indian Buffet Process (Griffiths & Ghahramani, 2011) prior on a feature matrix that encodes feature vector of nodes in its rows. (Foulds et al., 2011) proposed Dynamic Relational Infinite Feature Model (DRIFT) as an extension of LFRM for dynamic networks by allowing features of nodes to evolve under Markov assumption. While computing predictions for time t , LFRM model trained on time $t - 1$ was used (Foulds et al., 2011). Dynamic Multi-group Membership Model (DMMG) (Kim & Leskovec, 2013) uses a model similar to ours but with discrete node attributes and fixed interaction matrices (Section 2). All these methods use MCMC based inference but since our model is completely differentiable, we are able to use a neural network based variational inference procedure. (Gupta et al., 2019) also have a differentiable model for which they use neural network based variational inference, however, their generative model is restrictive as they only focus on assortative and undirected networks (Section 2).

We consider both directed and undirected networks. In the case of undirected networks the matrices $\Theta_k^{(t)}$ are symmetric for all $k = 1, 2, \dots, K$ and $t = 1, 2, \dots, T$, thus, effectively there are only three random variables in each $\bar{\theta}_k^{(t)}$. A simple change to the output dimension of the relevant GRUs (\mathcal{G}_m^θ and $\mathcal{G}_\sigma^\theta$ in Appendix B) accommodates this.

We use the well known AUC (Area Under Curve) score for comparison with other approaches. AUC computes the area under the true-positive rate vs false-positive rate curve for various values of threshold used for classification. Values close to 1 indicate good results. The scores reported in Tables 2 and 3 were obtained by first averaging the scores obtained across snapshots and then taking the mean values across 20 independent runs of the inference network.

We were not able to obtain an implementation for DMMG and therefore we present only the values reported by the authors in (Kim & Leskovec, 2013). It can be seen that our approach outperforms all the other approaches on all datasets except Infocom. We believe that this is because the Infocom network changes quickly across snapshots as it is a contact network and it has abrupt breaks (at the end of each day when participants leave the premises). This violates our assumption of a slowly changing network.

5.2 Qualitative Analysis

In this section, we present some qualitative insights about NIPS-110 and MIT Reality Mining datasets that were revealed by our model. For NIPS-110, author

Table 2: Link forecasting - Mean AUC scores with standard deviation across 20 independent executions of the experiment for undirected networks

	Enron-50	Infocom	NIPS-110	EU-U
BAS	0.874	0.698	0.703	0.914
LFRM (MILLER ET AL., 2009)	0.777	0.640	0.398	-
DRIFT (FOULDS ET AL., 2011)	0.910	0.782	0.672	-
DMMG (KIM & LESKOVEC, 2013)	-	0.804	0.732	-
iELSM (GUPTA ET AL., 2019)	0.913	0.868	0.754	0.948
DLAIM (THIS PAPER)	0.923 ± 0.002	0.821 ± 0.007	0.810 ± 0.008	0.973 ± 0.001

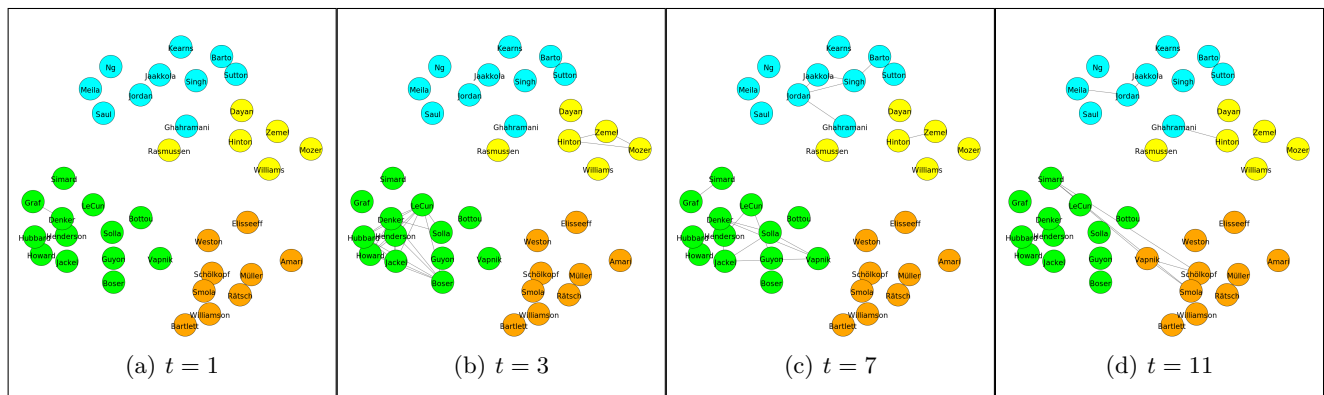


Figure 1: [Best viewed in color] Network between a subset of authors chosen to highlight the community structure. Different colors have been used to differentiate the communities found by running spectral clustering algorithm on a normalized version of adjacency matrix predicted by our method.

Table 3: Link forecasting - Mean AUC scores with standard deviation across 20 independent executions of the experiment for directed networks

	BAS	DLAIM (THIS PAPER)
Enron-Full	0.842	0.928 ± 0.004
EU-D	0.902	0.934 ± 0.003
CollegeMsg	0.686	0.857 ± 0.007

names were obtained by parsing the raw data³ and selecting top 110 authors as before. We use $K = 8$ for this analysis. A smaller value of K was chosen to aid the manual inspection process.

As ground truth communities are available for MIT Reality Mining dataset, we used it for a sanity check. It is known that two communities that align with ground truth communities can be discovered from the network structure (Xu & Hero, 2014; Eagle et al., 2009). We followed the same procedure as in (Xu & Hero, 2014) and our model was able to recover both communities. We also observed that both node at-

³http://www.cs.huji.ac.il/~papushado/nips_collab_data.html

tributes and interaction matrices evolved with time.

For NIPS-110 dataset, we observed that node attributes for authors did not change noticeably over time, however, the interaction matrices showed time dependent behavior. This aligns with what one might intuitively expect: authors typically do not dramatically change their domain of expertise over time, but they may start collaborating with different people as connections among different fields emerge.

We further conducted two experiments. First, we trained our inference network on all available snapshots and performed community detection on all snapshots using the trained embeddings. Second, we incrementally trained $T - 2$ inference networks (starting by observing only two snapshots for the first network and going up to observe $T - 1$ snapshots for the last network), and then performed community detection on the first snapshot using embeddings for first snapshot obtained from each of the $T - 2$ trained networks.

To perform community detection at a given timestep t , we use the learned embeddings to compute the summation term inside $\sigma(\cdot)$ in (1) for all pair of nodes to get $\tilde{\mathbf{A}}^{(t)}$. We mean normalize entries of $\tilde{\mathbf{A}}^{(t)}$, exponentiate them and then perform spectral clustering on this

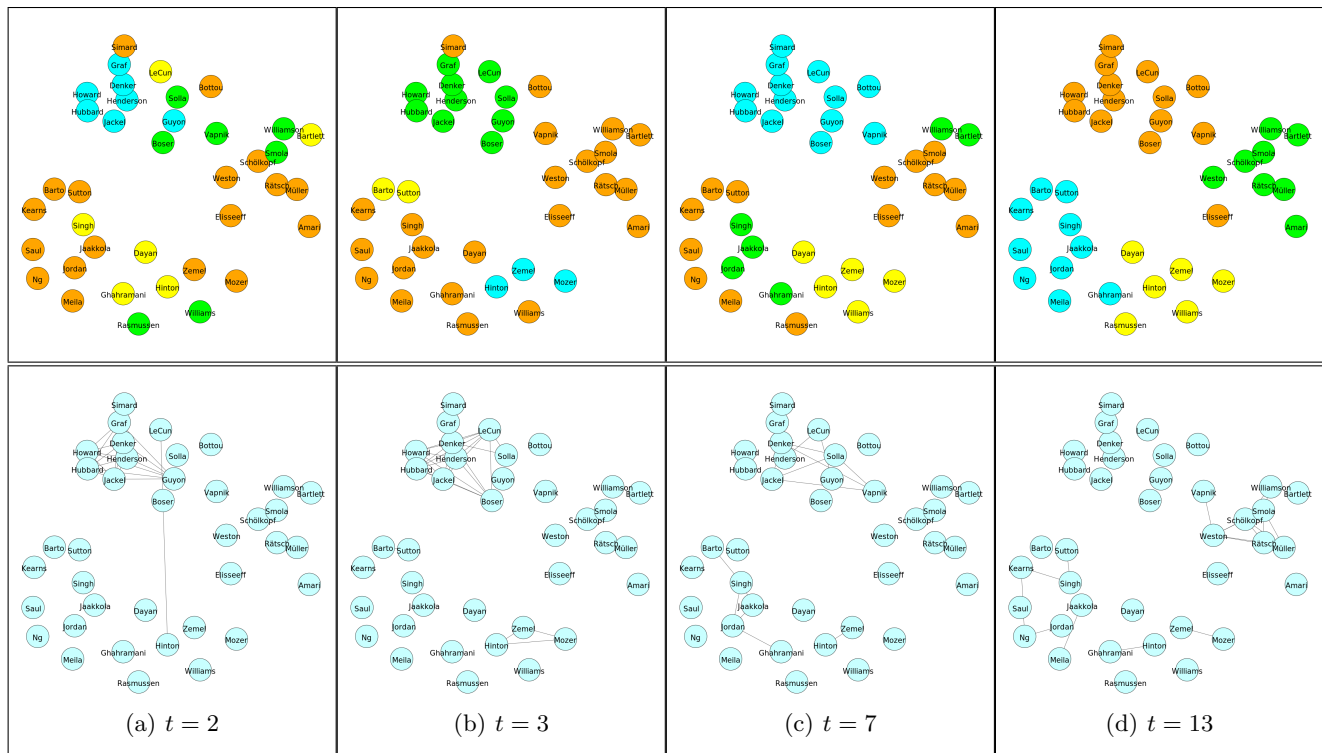


Figure 2: [Best viewed in color] First row depicts the outcome of community detection on the first time step. Second row shows the last adjacency matrix observed by the corresponding inference network that was used to provide embeddings for performing community detection in first row.

matrix. We chose spectral clustering as it can possibly discover non-convex clusters. Note that this is different from clustering on all snapshots independently since the embeddings capture temporal smoothness.

Through the first experiment, we wish to demonstrate that learned embeddings enforce smoothness over model dynamics (Fig 1). In Fig 1(a), nodes have been classified into communities because they will coauthor a paper together in future, despite having no edges between them at $t = 1$ (see Fig 1(b) and 1(c)).

It might appear that nodes do not switch communities at all and that same result would have been obtained by running spectral clustering on the sum of all snapshots. However, this is not true. One can see that Vapnik is part of green community at $t = 7$ and orange community at $t = 11$ since after that time he publishes multiple papers with members from orange community. This demonstrates that our method captures temporal smoothness while being flexible enough to capture temporal changes.

Through the second experiment, we wish to demonstrate how learned embeddings from past are updated as new information arrives. It can be seen in Fig 2 that as new edges are observed in future, embeddings for first time step are updated to reflect this informa-

tion. As an example, Hinton, Williams, Zemel and Rasmussen belong to different communities when only the first two snapshots have been observed, but over time these authors become part of the same community as they publish papers together. Note that the first row in Fig 2 corresponds to $t = 1$ for all columns, hence, new information has to temporally flow backward for Fig 2 to emerge.

6 CONCLUSION

In this paper, we presented a new statistical model for dynamic networks along with an associated neural network based variational inference procedure. The proposed model not only does not impose strict restrictions on the dynamics of networks, but is also applicable to a large class of directed as well as undirected networks. We demonstrated the utility of our approach by using it to perform link forecasting where we achieved state-of-the-art performance. A qualitative study provides further evidence that the learned latent quantities might carry useful information.

We briefly mentioned how our proposed model can accommodate a change in number of nodes in Appendix D. One can also explicitly model a variable number of attributes as done in (Kim & Leskovec, 2013).

References

- Airoldi, E. M., Blei, D. M., Fienberg, S. E., and Xing, E. P. Mixed membership stochastic blockmodels. *Journal of Machine Learning Research (JMLR)*, 9:1981–2014, 2008.
- Bengio, Y., Simard, P., and Frasconi, P. Learning long-term dependencies with gradient descent is difficult. *IEEE Transactions on Neural Networks*, 5(2):157–166, 1994.
- Blei, D. M., Kucukelbir, A., and McAuliffe, J. D. Variational inference: A review for statisticians. *Journal of the American Statistical Association*, 112(518):859–877, 2017.
- Cho, K., van Merriënboer, B., Bahdanau, D., and Bengio, Y. On the properties of neural machine translation: Encoder-decoder approaches. *Eighth Workshop on Syntax, Semantics and Structure in Statistical Translation (SSST-8), 2014*, 2014.
- Eagle, N. and Pentland, A. S. Reality mining: sensing complex social systems. *Journal Personal and Ubiquitous Computing*, 10(4):255–268, 2006.
- Eagle, N., Pentland, A. S., and Lazer, D. Inferring friendship network structure by using mobile phone data. *Proc. Natl. Acad. Sci.*, 106(36):15274–15278, 2009.
- Foulds, J., DuBois, C., Asuncion, A., Butts, C., and Smyth, P. A dynamic relational infinite feature model for longitudinal social networks. *Proceedings of Machine Learning Research (PMLR)*, 15:287–295, 2011.
- Goldenberg, A., Zheng, A. X., Fienberg, S. E., and Airoldi, E. M. A survey of statistical network models. *Foundations and Trends in Machine Learning*, 2(2):129–233, 2010.
- Griffiths, T. L. and Ghahramani, Z. The indian buffet process: An introduction and review. *Journal of Machine Learning Research (JMLR)*, 12:1185–1224, 2011.
- Gupta, S., Sharma, G., and Dukkipati, A. A generative model for dynamic networks with applications. In *Proceedings of Thirty-Third AAAI Conference on Artificial Intelligence (AAAI)*, 2019.
- Heaukulani, C. and Ghahramani, Z. Dynamic probabilistic models for latent feature propagation in social networks. In *Proceedings of the 30th International Conference on International Conference on Machine Learning*, volume 28, pp. I–275–I–283, 2013.
- Hochreiter, S. and Schmidhuber, J. Long short-term memory. *Neural Comput.*, 9(8):1735–1780, 1997.
- Holland, P. W., Laskey, K. B., and Leinhardt, S. Stochastic blockmodels: First steps. *Social Networks*, 5(2):109 – 137, 1983.
- Kim, B., Lee, K., Xue, L., and Niu, X. A review of dynamic network models with latent variables. *CoRR*, 2017.
- Kim, M. and Leskovec, J. Multiplicative attribute graph model of real-world networks. *Internet Mathematics*, 8(1-2):113–160, 2012.
- Kim, M. and Leskovec, J. Nonparametric multi-group membership model for dynamic networks. *Advances in Neural Information Processing Systems*, 26:1385–1393, 2013.
- Kingma, D. P. and Ba, J. Adam: A method for stochastic optimization. *Proceedings of 3rd International Conference on Learning Representations (ICLR)*, 2014.
- Kingma, D. P. and Welling, M. Auto-encoding variational bayes. *Proceedings of the 2nd International Conference on Learning Representations (ICLR)*, 2013.
- Klimt, B. and Yang, Y. The enron corpus: A new dataset for email classification research. *Machine Learning: ECML, Lecture Notes in Computer Science*, 3201, 2004.
- Miller, K., Jordan, M. I., and Griffiths, T. L. Non-parametric latent feature models for link prediction. *Advances in Neural Information Processing Systems*, 22:1276–1284, 2009.
- Panzarasa, P., Opsahl, T., and Carley, K. M. Patterns and dynamics of users’ behavior and interaction: Network analysis of an online community. *Journal of the American Society for Information Science and Technology*, 60(5):911–932, 2009.
- Sarkar, P. and Moore, A. W. Dynamic social network analysis using latent space models. *SIGKDD Explorations*, 7(2):31–40, 2005.
- Sewell, D. K. and Chen, Y. Latent space models for dynamic networks. *Journal of the American Statistical Association*, 110(512):1646–1657, 2015.
- Sewell, D. K. and Chen, Y. Latent space models for dynamic networks with weighted edges. *Social Networks*, 44:105 – 116, 2016.
- Xing, E. P., Fu, W., and Song, L. A state-space mixed membership blockmodel for dynamic network tomography. *The Annals of Applied Statistics*, 4(2):535–566, 2010.

Xu, K. S. Stochastic block transition models for dynamic networks. *Journal of Machine Learning Research (JMLR)*, 38:1079–1087, 2015.

Xu, K. S. and Hero, A. O. Dynamic stochastic block-models for time-evolving social networks. *IEEE Journal of Selected Topics in Signal Processing*, 8(4):552–562, 2014.

Yang, T., Chi, Y., Zhu, S., Gong, Y., and Jin, R. Detecting communities and their evolutions in dynamic social networks - a bayesian approach. *Machine Learning*, 82(2):157–189, 2011.

Yilmaz, A., Javed, O., and Shah, M. Object tracking: A survey. *ACM Comput. Surv.*, 38(4), 2006.

Yin, H., Benson, A. R., Leskovec, J., and Gleich, D. F. Local higher-order graph clustering. In *Proceedings of the 23rd ACM SIGKDD International Conference on Knowledge Discovery and Data Mining*, 2017.

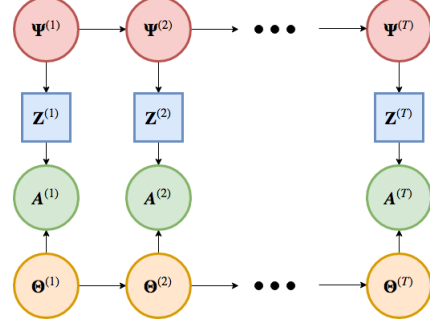


Figure 3: Graphical model for DLAIM. $\Psi^{(t)}$ are used to model node attributes and $\Theta^{(t)}$ represent the interaction matrices. Note that elements of $\mathbf{Z}^{(t)}$ are a deterministic function of the corresponding elements of $\Psi^{(t)}$.

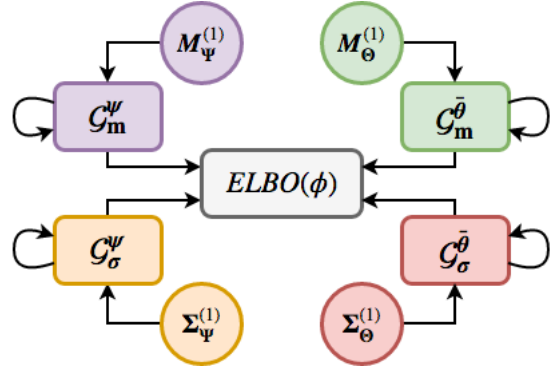


Figure 4: Inference Network Architecture. $\mathbf{M}_x^{(1)}$ and $\Sigma_x^{(1)}$ represent the initial learnable embeddings that are used by the respective GRUs \mathcal{G}_m^x and \mathcal{G}_σ^x . The output of all GRUs is used to compute ELBO.

A Algorithm for Generating Networks using DLAIM

The algorithm for generating dynamic networks using DLAIM is given in Algorithm 1. The graphical model is depicted in Fig. 3.

B Inference Network Architecture

We use a neural network to parameterize the distributions in (11) and (12). Our network consists of four separate GRUs (Cho et al., 2014) (see also Appendix C), one each for the mean and covariance parameters (\mathbf{m}_ψ , σ_ψ , \mathbf{m}_θ and σ_θ). We will refer to these GRUs as \mathcal{G}_m^ψ , \mathcal{G}_σ^ψ , \mathcal{G}_m^θ and $\mathcal{G}_\sigma^\theta$ respectively. These GRUs interact with each other only during the computation of $ELBO(\Phi)$ since their outputs are used to compute

Algorithm 1 Generative process for DLAIM

Input: N : Number of nodes,
 K : Number of attributes,
 T : Number of timesteps,
 s_θ^2 : Hyperparameter used in (3),
 s_ψ^2 : Hyperparameter used in (5),
 σ_θ^2 : Hyperparameter used in (6) and
 σ_ψ^2 : Hyperparameter used in (6)

Sample $\psi_n^{(1)}$ for $n = 1, 2, \dots, N$ and $\bar{\theta}_k^{(1)}$ for $k = 1, 2, \dots, K$ using (6)

for $t = 1$ **to** $T - 1$ **do**

Compute $\mathbf{z}_n^{(t)}$ by using $\psi_n^{(t)}$ in (4) for $n = 1, 2, \dots, N$

Sample $a_{ij}^{(t)}$ using (1) for $i, j = 1, 2, \dots, N, i \neq j$

Sample $\psi_n^{(t+1)}$ using (5) for $n = 1, 2, \dots, N$

Sample $\bar{\theta}_k^{(t+1)}$ using (3) for $k = 1, 2, \dots, K$

end for

Compute $\mathbf{z}_n^{(T)}$ by using $\psi_n^{(T)}$ in (4) for $n = 1, 2, \dots, N$

Sample $a_{ij}^{(T)}$ using (1) for $i, j = 1, 2, \dots, N, i \neq j$

Return: $[\mathbf{A}^{(1)}, \mathbf{A}^{(2)}, \dots, \mathbf{A}^{(T)}]$

(8). This has been depicted in Fig. 4.

For brevity of exposition, we will only describe the inputs and outputs for \mathcal{G}_m^ψ . For other GRUs, similar ideas have been employed. For $t = 1, 2, \dots, T - 1$, \mathcal{G}_m^ψ generates $\mathbf{m}_{\psi_n}^{(t+1)}$ at timestep t for all nodes in the current batch as output. In GRUs, the output of current timestep is used as the input hidden state for the next timestep, thus the input hidden state at timestep t corresponds to $\mathbf{m}_{\psi_n}^{(t)}$. To be consistent with this, the initial hidden state of \mathcal{G}_m^ψ should be $\mathbf{m}_{\psi_n}^{(1)}$. This means that the initial hidden state for \mathcal{G}_m^ψ is a learnable vector.

In all our experiments, we use an all 0's input vector for \mathcal{G}_m^ψ at each timestep. If observable features of nodes (that may be dynamic themselves) are available, one can instead use these features as input. For \mathcal{G}_σ^ψ and $\mathcal{G}_\sigma^\theta$, instead of computing the variance terms, which are constrained to be positive, we compute log of variance (this is again standard practice (Kingma & Welling, 2013)).

C Description of GRU

GRU or Gated Recurrent Unit is a type of recurrent neural network introduced by (Cho et al., 2014) in the context of natural language translation problem using neural networks.

Recurrent neural networks (RNN), as the name suggests, are designed to operate on inputs that are se-

quential in nature (for example, sentences, speech etc.). They maintain an internal state as a vector that is updated each time an input is received. This state is also used while processing the input tokens in a sequence. Unrolled along the time dimension, a standard recurrent neural network can be thought of as a very deep neural network. Due to this, standard RNNs suffer from the vanishing gradient problem where the gradients become too small to perform meaningful parameter updates thereby effectively stopping the learning process (Bengio et al., 1994). To overcome this problem, two popular variants of standard RNNs exist: LSTM (Hochreiter & Schmidhuber, 1997) and GRU (Cho et al., 2014). Since we use GRUs in our experiments we will describe the working of a GRU in this section.

Let $\mathbf{x}^{(t)} \in \mathbb{R}^d$ and $\mathbf{h}^{(t)} \in \mathbb{R}^k$ be the input vector and output hidden state respectively at time step t . The key idea is to be able to copy over information from previous time step if the current input token is not relevant for updating the state. Such an operation will counter the vanishing gradient problem as the derivatives for this operation will be close to the derivatives of an identity map. To achieve this, GRU computes a vector $\mathbf{z}^{(t)}$ at time t to act as an *update gate*:

$$\mathbf{z}^{(t)} = \sigma(\mathbf{W}_1 \mathbf{x}^{(t)} + \mathbf{W}_2 \mathbf{h}^{(t-1)}). \quad (13)$$

Here $\mathbf{W}_1 \in \mathbb{R}^{d \times k}$ and $\mathbf{W}_2 \in \mathbb{R}^{k \times k}$ are learnable parameters and $\sigma(x) = 1/(1 + \exp(-x))$ is the sigmoid function.

While retaining past information is useful, equally important is to forget the old information that is no longer needed. GRUs do this via the *reset gate*:

$$\mathbf{r}^{(t)} = \sigma(\mathbf{W}_3 \mathbf{x}^{(t)} + \mathbf{W}_4 \mathbf{h}^{(t-1)}). \quad (14)$$

As before, $\mathbf{W}_3 \in \mathbb{R}^{d \times k}$ and $\mathbf{W}_4 \in \mathbb{R}^{k \times k}$ are learnable parameters.

The output $\mathbf{h}^{(t)}$ at time t (which will also serve as input hidden state for time $t + 1$) is then computed as follows:

$$\mathbf{h}^{(t)} = \mathbf{z}^{(t)} \odot \mathbf{h}^{(t-1)} + (1 - \mathbf{z}^{(t)}) \odot \hat{\mathbf{h}}^{(t)}. \quad (15)$$

We use \odot for the elementwise multiplication operation and with \mathbf{W}_5 and \mathbf{W}_6 as learnable parameters:

$$\hat{\mathbf{h}}^{(t)} = \tanh(\mathbf{W}_5 \mathbf{x}^{(t)} + \mathbf{r}^{(t)} \odot \mathbf{W}_6 \hat{\mathbf{h}}^{(t-1)}). \quad (16)$$

In the context of our inference network, the input is always a zero vector although one may want to use node attributes as input if they are available. The initial hidden state $\mathbf{h}^{(0)}$ is itself a learnable parameter. At

time step t , the GRU takes the current value of variational parameter that it is modeling as input hidden state $\mathbf{h}^{(t-1)}$ and produces the variational parameter value for next time step as output at $\mathbf{h}^{(t)}$.

D Extension for Variable Number of Nodes

In this paper, our main focus is on networks where the number and identity of nodes do not change over time. However, our inference procedure is flexible enough to allow the number of nodes to vary over time. In this section, we briefly describe how this can be achieved. Although the number of nodes is allowed to change, we assume that the number of attributes is constant. We also assume that each node is *alive* only during a continuous time interval, in particular nodes are not allowed to reappear after disappearing.

Since the number of attributes is constant, there is no change in the way $\bar{\theta}_k^{(t)}$ is calculated for all k and t . The task then, is to find the vectors $\mathbf{m}_{\psi_n}^{(t)}$ and $\sigma_{\psi_n}^{(t)}$ for all nodes n that are alive at timestep t . We will mimic the procedure that was used in Section 4.2.

Suppose $[t_1, t_2]$ is the longest interval in which node i is alive, then $\psi_i^{(t_1)}$ will be drawn from the prior distribution given in (6). Note that $\psi_i^{(t)}$ does not exist for $t < t_1$ and $t > t_2$. For $t \in (t_1, t_2]$, $\psi_i^{(t)}$ follows (5). At timestep t , only those node pairs for which both nodes are alive at t , contribute to the last term in (9). Similarly, $\psi_i^{(t)}$ appears in the first and third term of (9) and first term of (10) only for $t \in [t_1, t_2]$.

Given a batch of nodes, the network architecture proposed in Appendix B can be used even in the case of variable number of nodes by using the appropriate terms to compute (8) and by treating appropriate vectors as learnable parameters as described above. We performed preliminary experiments by artificially assigning a birth time and death time to all nodes in the NIPS-110 dataset described in Appendix E. We were able to successfully train the inference network and get good performance on the link forecasting task. However, due to space constraints, we do not present our results here and leave detailed experiments for future work.

E Dataset Description

We use the following datasets in our link prediction experiments:

1. Enron email: The full Enron email corpus (Klimt & Yang, 2004) has 149 nodes corresponding to employees in a company. A directed edge from node i to node

j implies that i sent an email to j . We use an undirected subset of the Enron corpus (Enron-50) consisting of 50 nodes as described in (Foulds et al., 2011). We also perform link prediction on the full, directed Enron corpus with 149 nodes by taking data from years 2000-2001 where each network snapshot corresponds to a month (Enron-Full).

2. Infocom: There are 78 nodes in this network. An undirected edge from node i to node j at timestep t indicates that i and j were in proximity of each other during that timestep. We obtain a dynamic network with 50 snapshots by using the procedure outlined in (Gupta et al., 2019).

3. NIPS co-authorship: This dataset consists of 5,722 nodes. An undirected edge from node i to node j indicates that i and j co-authored a paper. We consider a subset of the dataset containing 110 nodes as described in (Heaukulani & Ghahramani, 2013). We refer to this dataset as NIPS-110.

4. EU Email: This dataset (Yin et al., 2017) contains information about emails that were exchanged between individuals belonging to an European research organization. There are 986 nodes in the network. We consider the first 495 days and create 33 network snapshots by aggregating data over 15 day time windows. We treat this as an undirected (EU-U) as well as a directed (EU-D) network.

5. ColleagueMsg: There are 1899 nodes in this dataset (Panzarasa et al., 2009). A binary, directed edge corresponds to a message exchanged between the sender and receiver. Temporal data for 193 days is available. We discard the last 3 days and divide the data into 10 days wide buckets which gives us 19 snapshots.

6. MIT Reality Mining: We use this dataset only for performing qualitative analysis in Section 5.2. This network has 94 nodes that correspond to people on MIT campus (Eagle & Pentland, 2006). Following (Xu & Hero, 2014), we aggregate the Bluetooth proximity data so that each snapshot corresponds to 1 week and we have 37 snapshots from August 2004 to May 2005.